10/4-4-97 JSD (1)

SANDIA REPORT

SAND95-8221 • UC–1409
Unlimited Release
Printed April 1995

M9705238 3

Four-Wave Mixing Using Polarization Grating Induced Thermal Grating in Liquids Exhibiting Circular Dichroism

J. A. Nunes, W. G. Tong, D. W. Chandler, L. A. Rahn

Prepared by
Sandia National Laboratories
Albuquerque, New Mexico 87185 and Livermore, California 94551
for the United States Department of Energy
under Contract DE-AC04-94AL85000

Approved for public release; distribution is unlimited.

MASTER

HH

DISTRIBUTION OF THIS DOCUMENT IS UNLIMITED

SAND95-8221
Unlimited Release
Printed April 1995

FOUR-WAVE MIXING USING POLARIZATION GRATING INDUCED THERMAL GRATING IN LIQUIDS EXHIBITING CIRCULAR DICHROISM

Jon A. Nunes and William G. Tong
Department of Chemistry,
San Diego State University
San Diego, California 92182
and
David W. Chandler and Larry A. Rahn
Combustion Research Facility
Sandia National Laboratory
Livermore, California 94551

ABSTRACT

A novel four-wave mixing technique for the detection of circular dichroism in optically active liquid samples is demonstrated. When two cross-polarized laser beams are crossed at a small angle in a circular dichroic liquid a weak thermal grating is produced with a phase depending on the sign of the circular dichroism. We show that the polarization of one of the beams can be modified to allow coherent interference with an intensity-grating induced thermal grating. A probe beam scattering from the composite grating results in a signal that reveals the sign and magnitude of the circular dichroism. The use of this technique to optimize the signal-to-noise ratio in the presence of scattered light and laser intensity noise is discussed.

ACKNOWLEDGMENT

We gratefully acknowledge support of this work from Sandia National Laboratories Office of Laboratory Directed Research and Development. The authors would like to thank Skip Williams for helpful discussions and John Laroco for technical assistance.

CONTENTS

FOUR-WAVE MIXING USING POLARIZATION GRATING INDUCED THERMAL GRATINGS IN LIQUIDS EXHIBITING CIRCULAR DICHROISM

Introduction

The laser has played a revolutionary role in the advancement and the development of modern optical diagnostic methods. It has improved many conventional techniques, while aiding in the creation of entirely new diagnostic practices that are only possible using laser light. An important example of a new technique is four-wave mixing (FWM), also commonly referred to as laser-induced grating spectroscopy (LIGS)[1]. FWM has proven to be a powerful tool for probing the chemical and physical properties of numerous different sample types. A particularly useful technique is degenerate four-wave mixing (DFWM) which has been demonstrated as a sensitive analytical spectroscopic method[2]. DFWM has been demonstrated in many different environments, including low-pressure hollow-cathode discharge cells[3-5], flame atomizers[6-9], and liquid flow cells[10,11]. In the gas phase, sub-Doppler spectral resolution allows hyperfine structure measurement and stable isotope ratio analysis at trace concentrations[9]. For condensed-phase analytes, attomole-level detection sensitivity has been obtained using continuously flowing liquid cells[12]. Two-color variants of DFWM has been used for gas-phase excited state spectroscopy[13,14], for measurements of small absorptions in liquids[15,16], and to investigate molecules in free-jet expansions[17]. These methods offer unique advantages over many conventional optical spectroscopic techniques including laser-limited resolution, convenient and efficient optical signal collection on a "zero" background and excellent detection sensitivity.

It is these advantages that drove Nunes and Tong[18] to develop a DFWM technique to measure circular dichroism (CD), the differential absorption of right- and left-handed circularly polarized light that chiral molecules exhibit. CD spectroscopy is an optical method for analyzing the chirality of molecules. It has become the method of choice[19] over polarimetry and optical rotary dispersion for the study of inorganic and organic molecular structural configurations[20], the study of conformational properties of proteins[21], and the analytical detection of optically active substances[22-24]. Nunes and Tong demonstrated for the first time CD measurements made by using a forward scattering degenerate four-wave

mixing (F-DFWM) geometry and were able to make sensitive CD measurements by employing a Pockels cell for polarization modulation.

In this paper we investigate the use of a four-wave mixing (FWM) technique to detect circular dichroism of liquid samples. With FWM the observed signal is produced by scattering a probe laser from the effects of a thermal grating in the sample induced by periodic variations in absorption in the intersection volume of two coherent excitation laser beams. When the excitation beams are of the same polarization, an intensity modulation is produced at their intersection and any absorption results in a thermal grating. When the excitation beams are *cross* polarized, however, only the polarization is modulated at their intersection and there is normally no thermal grating produced. In samples that exhibit circular dichroism a weak thermal grating is produced with cross-polarized beams because the absorption is polarization dependent. Nonchiral samples do not produce such a signal. We show that the polarization of one of the cross-polarized beams can be modified to allow coherent interference with an intensity-grating induced thermal grating. A probe beam scattering from the composite grating results in a signal that reveals the sign and magnitude of the circular dichrosim. The use of this technique to optimize the signal-to-noise ratio in the presence of scattered light and laser intensity noise is discussed. We also discuss the potential advantages of using this technique to make CD measurements compared to conventional methods.

Theory of Operation

Circular dichroism. CD is defined as the difference in absorbance of left circularly polarized light (LCPL) and right circularly polarized light (RCPL). The absorption-based CD signal can be described in terms of molar absorptivities for LCPL and RCPL as:

$$\Delta\varepsilon = \varepsilon_L - \varepsilon_R \qquad (1)$$

where ε_L and ε_R are the molar absorptivities for LCPL and RCPL, respectively, and $\Delta\varepsilon$ is the differential molar absorptivity. Equation 1 can be related to conventional absorbance measurements by substitution into the Beer-Lambert law,

$$\Delta A = A_L - A_R = \Delta\varepsilon bC = \varepsilon_L bC - \varepsilon_R bC \qquad (2)$$

where b is path length (cm), C is concentration (M), A_L and A_R are the absorbance for LCPL and RCPL, respectively, and ΔA is the differential absorbance.

Four-Wave Mixing. FWM is a process that can, among other ways, be described in terms of the creation and scattering from laser induced gratings.[1] The spatially (and possibly temporally) modulated electric field resulting from the interference between two crossed excitation or pump beams affects the optical properties of a medium. A signal is generated when a third probe beam is diffracted from the modulation grating induced by the pump beams. This picture is especially useful in cases where thermal gratings are the important mechanism, as they are in the present work. The relation of the grating picture to that of the nonlinear optical susceptibility has been discussed by Fourkas, et al.[25]

The experimental geometry used in this work is depicted in Figure 1. We consider two intersecting coherent excitation laser beams of wavelength λ_{ex} intersecting at an angle a. The laser-induced grating modulation at the intersection is transverse to the excitation beams and has a spacing given by

$$d = \lambda_{ex} / 2\sin(\alpha/2). \qquad (3)$$

The direction of the probe laser is typically determined by phase-matching conditions. In our case, the path length through the sample cell is so short, (0.5 mm), that the probe beam can be directed into the sample at any angle as long as it is overlapped with the grating excitation beams. This Raman-Nath or "thin grating condition" [26] produces scattering of the probe beam into multiple diffraction orders, one of which is directed into the detection system.

Thermal Gratings. A thermal grating can be generated when two laser beams are crossed at a small angle inside an absorbing liquid. Crossed beams with the same linear polarizations create an intensity pattern (an intensity grating) in the crossover region of the two beams. The pattern resembles a conventional diffraction grating composed of light and dark interference fringes. This intensity modulation can be imprinted on the absorbing medium in the form of a thermal modulation or "thermal grating" that is spatially coherent with the intensity pattern. Absorption and subsequent radiationless relaxation in the sample produces a thermal grating with higher temperature fringes aligned with the higher intensity fringes in an intensity grating. The temperature fluctuations result in corresponding spatial modulations in the refractive index which act as a phase grating[1]. It is this spatially nonuniform refractive index that scatters the impinging probe beam. This process for parallel polarizations is depicted in Figure 2a, where the top portion shows the resultant

grating electric field and the bottom section represents the thermal response by the absorbing sample.

When the same crossed input beams have perpendicular linear polarizations, a very different situation arises. No longer can the two beams interfere to form an intensity pattern. Since in this case there is no generated intensity pattern, there can be no intensity-grating-induced thermal grating. This is easily demonstrated experimentally by rotating the electric field polarization of one the pump beams in a thermal grating experiment by 90°. The observed scattering is completely quenched when the pump polarizations are exactly orthogonal.

CD-induced Thermal Gratings. There is, however, a way in which cross-polarized laser beams can produce a thermal grating in a liquid that exhibits circular dichroism. The interference pattern drawn at the top of Figure 2b shows how the resultant electric field in the pump beam crossover region changes in polarization, but not in magnitude across one grating fringe. The polarization changes from right circular to linear to left circular to linear (90° shifted) and back to right circular. In between these polarization states are the corresponding transitional elliptical polarizations[25]. Thus, a "polarization grating" superimposed upon an absorbing chiral compound exhibiting circular dichroism results in a thermal grating (Figure 2b, bottom) produced by the differential absorption of right and left circularly polarized light (CPL). This can be illustrated as follows. Consider an optically active sample that possesses a $\Delta\varepsilon$ that is negative, i.e. it absorbs RCPL more than LCPL. Figure 2b shows the difference in absorption across one grating fringe (from $x = 0$ to $x = d$). It is apparent that at $x = 0$, where the electric field polarization is RCP, there is maximum absorption by the sample. At $x = d/2$, where the electric field polarization is LCP, there is a minimum in the sample absorption. Finally, at $x = d$ the polarization is again RCP and the sample absorption is again at its highest point. This differential absorption results in a non uniform spatial temperature distribution, i.e. a thermal grating. This thermal grating, although weak, can result in a scattered signal detectable with a photomultiplier tube.

Further study reveals that the polarization of one the beams can be modified to allow coherent interference of a CD-induced thermal grating (CDTG) with an intensity-grating induced thermal grating (IGTG). Notice that a CD-induced thermal grating is 90°

(d/4) spatially phase shifted relative to an intensity grating induced thermal grating as shown in Figure 2. The direction of the shift depends on the sign of $\Delta\varepsilon$ of the particular sample under investigation. If $\Delta\varepsilon$ has a positive sign, the sample absorbs LCPL more then RCPL and the absorption maxima will thus be at the LCP regions of the polarization grating. If $\Delta\varepsilon$ is negative the opposite is true. By introducing a 90° phase shifted IGTG it is possible to coherently interfere both thermal gratings in the sample. This process is schematically depicted in Figure 3. Two representations of a polarization grating are shown in Figure 3a. The top section is an electric field picture similar to that shown in Figure 2 with only the circular portions drawn, and below that is an optical field representation. The optical field drawing conveniently shows the spatial transition between the left and right circular polarizations across the grating. Figure 3b shows how the introduction of a normal (i.e., no phase shift) IGTG is out of phase with the polarization grating. However, if an IGTG that is 90° phase shifted is added, as shown in Figure 3c, the two gratings are now correctly positioned to interfere. When a chiral substance that has a positive $\Delta\varepsilon$ (more absorption of LCP then RCP) is under investigation, this IGTG would destructively interfere with the corresponding CDTG. If the correct amplitude of IGTG is added, complete grating cancellation would occur and the scattered signal will disappear. In the case of a chiral substance with a negative $\Delta\varepsilon$ constructive interference occurs causing the signal to increase in intensity. Figure 3d shows an IGTG profile for an opposite phase shift.

Experimentally the described interference processes can be achieved by placing a quarter-wave retarder in one of the excitation pump beams and slightly rotating it. It can be shown[28] that this rotation is directly related to the ratio of the samples circular dichroism ($\Delta\varepsilon$) to the overall average absorption coefficient (ε) such that

$$\Theta \text{ (radians)} = \Delta\varepsilon / \varepsilon. \qquad (4)$$

Figure 4 is a theoretical plot of the average signal verses rotation for a (+) and (-) chiral sample. Depending on the sign of $\Delta\varepsilon$, a minimum occurs in the signal when the rotation is at $\Theta = \Delta\varepsilon / \varepsilon$. In the present work these minimums are experimentally determined for separate enantiomers of a chiral substance and compared to calculated values.

Experimental

The FWM experimental arrangement is shown in Figure 5. Gratings are formed using a single mode CW argon ion laser (Spectra Physics, Model 171) operating at 488 nm. The laser output is split into two beams using a 50/50 beam splitter and recombined at the 0.5 mm path length liquid flow cell. One of the two pump beams passes through a mechanical chopper, operated at a frequency of 250 Hz that is part of the amplitude modulation scheme for lock-in detection of the signal, then through a calcite polarizer to ensure "pure" linear polarization. The other beam passes through a calcite polarizer and then passes through a half-wave plate that is used to control the type of grating that is prepared in the sample solution. When the wave plate has its crystal axis aligned with the beam polarization axis there is no polarization rotation and hence both beams have parallel polarization. With this configuration an intensity grating is formed in the sample. When the wave plated is rotated 45° the beams are crossed polarized and a polarization grating is generated.

A 1.5 mW HeNe laser operating at 632 nm is used as a probe laser. The HeNe probe beam is introduced below the plane created by the argon pump waves and is diffracted by the grating into two signal beams. One of the red diffracted beams is passed though a blue color filter, a 250 μm pinhole, a 632 nm laser line filter, and finally to a PMT for detection. The amplitude modulated signal is sent to a lock-in amplifier that is frequency referenced to the mechanical chopper. The demodulated signal is recorded on a chart recorder and a personal computer.

Optically active (+) and (-) tris(ethylenediamine)cobalt (III) complexes, (+)$[Co(en)_3]I_3$and (-)$[Co(en)_3]I_3$, are synthesized and prepared using standard methods[27]. Racemic mixture solutions of these enantiomers are also prepared. All solutions are prepared using a water:ethanol solvent mixture (1:1 by volume), and used immediately after preparation. Non optically active samples of $CoSO_4$ and $CoCl_2$ are also prepared in order to use as standards. All solvents are filtered before they are used (0.2 μm).

Discussion of Results

CD Signals. A half-wave plate in one of the input pump beams allows selection of the type of grating that is generated in the sample, either intensity, polarization, or a combination of the two. Data collection consists of monitoring the signal intensities for

different samples while changing between gratings (i.e., rotating the half-wave plate). The ratio of the signal intensity from the polarization grating scheme (crossed pump polarizations) and the signal intensity from the intensity grating scheme (parallel pump polarizations) is the main focus for each individual sample. This ratio is more meaningful than comparing absolute polarization grating signal intensities, since this ratio is immune to day-to-day experimental variances (laser power, alignment, etc.). Ratio comparisons between chiral and nonchiral samples is the superior method to verify that the scattered signals truly result from circular dichroism effects and not polarization impurities.

When the input pump beams have parallel linear polarizations, strong, equal intensity scattering signals are observed for the three equivalently concentrated $Co(en)_3^{3+}$ samples. These signals are expected to be identical for these solutions, since the resultant field in the beam crossover zone that creates the intensity-induced thermal grating has an unvarying polarization. However, when the two argon pump beams are cross polarized, the results are different. In this case a polarization grating is formed where the resultant field across the grating changes in polarization as described earlier. When the same three samples are probed in this configuration, scattering signals are observed only for the $(+)Co(en)_3^{3+}$ and $(-)Co(en)_3^{3+}$ solutions. No signal is detected for the racemic mixture. Also tested were samples of $CoSO_4$ and $CoCl_2$. These compounds absorb similarly to $Co(en)_3^{3+}$ at the 488 nm argon ion laser excitation wavelength, but are not optically active. Strong FWM signals are observed for both samples when the pump beam polarizations were parallel, but as expected no signals are detected for perpendicularly polarized pump beams above the scattered light noise.

Table 1 exhibits a comparison between calculated and experimental dissymmetry ratios, $\Delta\varepsilon/\varepsilon$, for the two $Co(en)_3^{3+}$ enantiomers. The calculated ratios were determined using $\varepsilon = 81$ and $\Delta\varepsilon = 0.6$ L cm^{-1} mol^{-1}. Both these values were experimentally measured for the solutions of $Co(en)_3^{3+}$ using commercial UV-Vis absorption and CD spectrometers. The experimental dissymmetry ratios were determined using

$$\frac{\Delta\varepsilon}{\varepsilon} = \left(\frac{S_{\perp}}{S_{\parallel}}\right)^{\frac{1}{2}} \qquad (5)$$

where $S_{\perp}$ and $S_{\parallel}$ are the signal intensities for perpendicular (polarization grating) and parallel (intensity grating) polarized pump beams, respectively. As shown in Table 1, the

theoretical and experimental values are in good agreement with one another. The discrepancy between the experimental and theoretical results can be attributed primarily to the difficulty involved in measuring $S_{\perp}$. Since this signal is very small, it is often eclipsed by stray probe laser light. Micropinhole spatial filtering is necessary for the signal to be measured accurately.

Directly determining $\Delta\varepsilon/\varepsilon$ by grating interference. As described earlier it is possible to distinguish between different enantiomers by "mixing" a CD-induced thermal grating and an intensity-induced thermal grating. In our experiments the intensity grating is produced by placing a quarter-wave retardation plate into one of the pump beams. With the pump beam polarizations crossed and the quarter-wave plate inserted with its optic axis parallel to the beam polarization, the scattered signal remains essentially unchanged. Upon a small rotation of the waveplate in one direction the signal intensity drops to the observed baseline. At this point the phase shifted IGTG is 180° out of phase with the CDTG and scattering from a thermal grating is minimized (see Figure 4). If the waveplate is rotated an equal amount in the opposite direction relative to the optic axis, the observed signal rises, indicating that the IGTG is constructively interfering with the CDTG. When the sample is changed to the opposing enantiomer, the polarizations reverse. An equal, but opposite rotation is required to minimize the signal.

The magnitude and sign of the quarter-wave plate rotation that is required to quench the CDTG can be calculated using equation (4) where Θ (in radians) is the amount of quarter-wave plate rotation required to minimize the signal. Table 1 lists the calculated rotation angles as well as the experimentally observed results for the two enantiomers studied. The theoretical and experimental values are again in good agreement with one another.

Future Work. The method described in this work is similar to the DFWM-CD technique, but it does have some interesting and significant differences and advantages. A fundamental difference is that with this method the CD signal is on a true zero background and is not based on subtraction modulation techniques to derive the signal, since there is only scattering if a chiral sample is present. This basic distinction therefore eliminates the need for any type of polarization modulation in the experimental setup, thereby having the

potential for dramatically simplifying making CD measurements. Further technical advantages include the methods potential for use with short path length sample cells and ultra-small probe volumes, because the probing light comes from a laser and can be tightly focused. Hence the potential use with analytical separation techniques (i.e. liquid chromatography or capillary electrophoresis) is provided.

Although CD measurements with this FWM-CD technique are unique and straightforward, the method suffers from stray probe laser light and polarization impurity problems that obscure the signal. With especially small CD values this becomes very significant, since the measured signal has a squared dependence on the $\Delta\varepsilon/\varepsilon$ ratio. Further investigations are underway to improve the technique by combining this method and that described by Nunes and Tong[18]. By strategically combining polarization gratings and intensity gratings using a dynamic polarization device (such as a photoelastic modulator) it should be possible to "amplify" the CD response similar to that done in heterodyne techniques used in Raman and frequency modulation spectroscopies. This grating combination would entail modulating between the situations shown in Figure 3c and Figure 3d. This method is currently being developed for CD detection in the ultraviolet using pulsed laser excitation.

REFERENCES

1. Eichler, H. J.; Gunter, P.; Pohl, D. W. *Laser-Induced Dynamic Gratings*, Springer-Verlag, 1986.
2. Farrow, R. L.; Rakestraw, D. J. *Science*, 1992, 257, 1894-1900.
3. Tong, W. G.; Chen, D. A. *Applied Spectroscopy* 1987, 41, 586-590.
4. Chen, D. A.; Tong, W. G. *J. Anal. Atom. Spectrom.* 1988, 3, 531-535.
5. Wu, Z.; Tong, W. G. *Spectrochimica Acta B* 1992, 47B, 3, 449-457.
6. Tong, W. G.; Andrews, J. M.; Wu, Z. *Analytical Chemistry* 1987, 59, 896-899.
7. Andrews, J. M.; Tong, W. G. *Spectrochimica Acta 1989,* 44B, 101-107.
8. Andrews, J. M.; Weed, K. M.; Tong, W. G. *Applied Spectroscopy* 1991, 45, 697-700.
9. Wu, Z.; Tong, W. G. *Analytical Chemistry* 1991, 63, 899-903.
10. Wu, Z.; Tong, W. G. *Analytical Chemistry* 1989, 61, 998-1001.
11. Wu, Z.; Tong, W. G. *Analytical Chemistry* 1991, 63, 1943-1947.
12. Wu, Z.; Tong, W. G. *Analytical Chemistry* 1993, 65, 112-117.
13. Buntine, M. A.; Chandler, D. W.; Hayden, C.C. *J. Chem. Phys.* 1992, 97, 1, 707-710.
14. Gray, J. A.; Goldsmith, J. E. M.; Trebino, R. *Opt. Lett.* 1993, 18, 6, 444-446.
15. Harris, J. M.; Pelletier, M. J.; Thorshelm, H. R. *Analytical Chemistry* 1982, 54, 239-242.
16. Harris, J. M.; Pelletier, M. J. *Analytical Chemistry* 1983, 55, 1537-1543.
17. Butenhoff, T. J.; Rohlfing, E. A. *J. Chem. Phys.* 1992, 97, 1595-1602.
18. Nunes, J. A.; Tong, W. G. *Anal. Chem.* 1993, 65, 2990-2994.
19. Purdie, N.; Swallows, K. A. *Anal. Chem.* 1989, 61, 77A-89A.
20. Nakanishi, K.; Kuroyanagi, M.; Nambu, H.; Oltz, E. M.; Takeda, R.; Verdine, G. L.; Zask, A. *Pure Appl. Chem.* 1984, 56, 1031-1048.
21. Carrara, E. A.; Gavotti, C.; Catasti, P.; Nozza, F.; Berutti Bergotto, L. L.; Nicolini, C. A. *Arch. Biochem. Biophys.* 1992, 294, 107-114.
22. Drake, A. F.; Gould, J. M.; Mason, S. F. *J. Chromatogr.* 1980, 202, 239-245.
23. Westwood, S. A.; Games, D. E.; Sheen, L. *J. Chromatogr.* 1981, 204, 103-107.
24. Premuzic, E. T.; Gaffney, J. S. *J. Chromatogr.* 1983, 262, 321-327.
25. Fourkas, J. T.; Trebino, R.; Fayer, M. D. *J. Chem. Phys.* 1992, 97, 1, 69-77.
26. Moharam, M. G.; Gaylord, T. K.; Magnusson, R. *Optics Comm.* 1980, 32, 19-23.
27. Angelici, R. J. *Synthesis and Techniques in Inorganic Chemistry,* W. B. Saunders Co., Philadelphia, 2nd ed., 1977.
28. Neyer, D. W., Nunes, J. A., Tong, W. G., Rahn, L. A., and Chandler, D. W., in preparation.

FIGURE CAPTIONS

Figure 1. Three and two dimensional representations of the four-wave mixing geometry used in the experiment. The two pump waves, E_{p1} and E_{p2}, are in the same plane and have crossed polarizations with respect to one another. The thin grating scatters the probe beam E_{probe} into two signal beams, $E^{+1}{}_s$ and $E^{-1}{}_s$.

Figure 2. Relative phases of gratings relevant to this experiment.

(a) Pump beams with parallel polarizations create an intensity grating, i.e. the resultant electric (top portion) field varies in intensity across the grating. In an absorbing medium a thermal grating (lower) is formed.

(b) Pump beams with crossed polarizations create a polarization grating where the resultant field varies in polarization, but not in intensity across the grating. In a chiral sample this polarization grating gives rise to a CD-induced thermal grating where the grating peaks and troughs correspond to the different circular polarizations across the polarization grating fringes. Note that the intensity-induced thermal grating and the CD-induced thermal grating are 90° out of phase.

Figure 3. Phase representation of circular dichroism-induced thermal grating (CDTG) and intensity grating induced thermal grating (IGTG) interference.

(a) Polarization grating shown in an electric field representation with only the circular portions drawn (top) and an optical field representation (lower).

(b) A normal (i.e., unshifted) intensity grating is 90° out of phase with the polarization grating.

(c) A 90° phase shifted intensity grating will produce a thermal grating that will interfere with a CDTG. A sample with a positive $\Delta\varepsilon$ will result in a grating that destructively adds to the phase shifted IGTG. A negative $\Delta\varepsilon$ results in constructive interference.

(d) An IGTG with the opposite phase shift reverses the resulting interferences for the different samples.

Figure 4. Theoretical plot of the average FWM signal verses quarter wave plate rotation for a (+) and (-) chiral sample. Depending on the sign of $\Delta\varepsilon$, a minimum occurs in the signal when the rotation is at $\Theta = \Delta\varepsilon / \varepsilon$.

Figure 5. Four-wave mixing circular dichroism experimental setup.

Table 1: Theoretical and Experimental Results of Circular Dichroism Measurements Using CD-Induced Thermal Gratings

	Theoretical Values		**Experimental Values**	
Sample	**Dissymmetry Ratio**	**Rotation Angle**	**Dissymmetry Ratio**	**Rotation Angle**
$(+)Co(en)_3^{3+}$	7.4×10^{-3}	+0.41°	5.1×10^{-3}	+0.4°
$(-)Co(en)_3^{3+}$	-7.4×10^{-3}	-0.41°	6.2×10^{-3}	-0.5°

3D Geometrical Representation

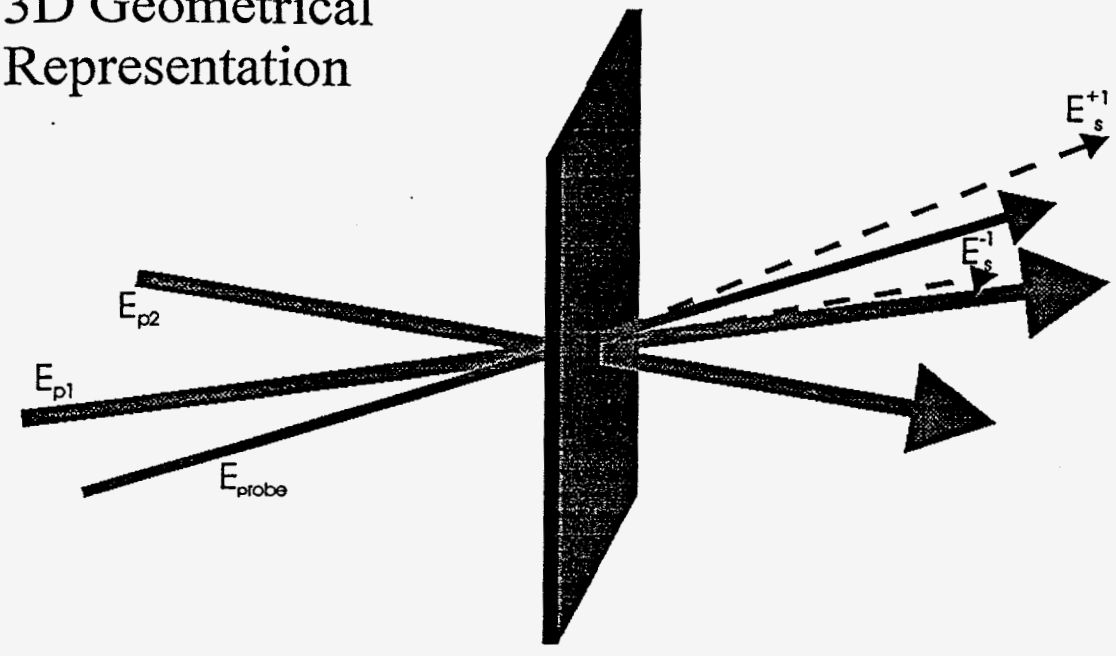

2D Geometrical Representation

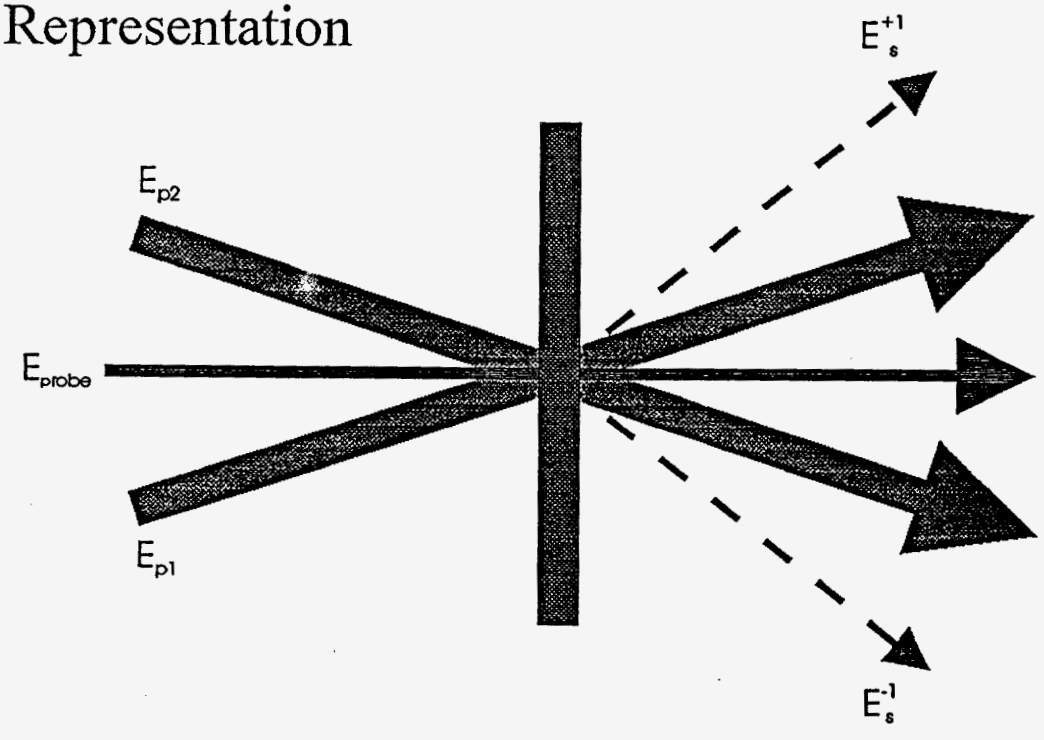

Figure 1

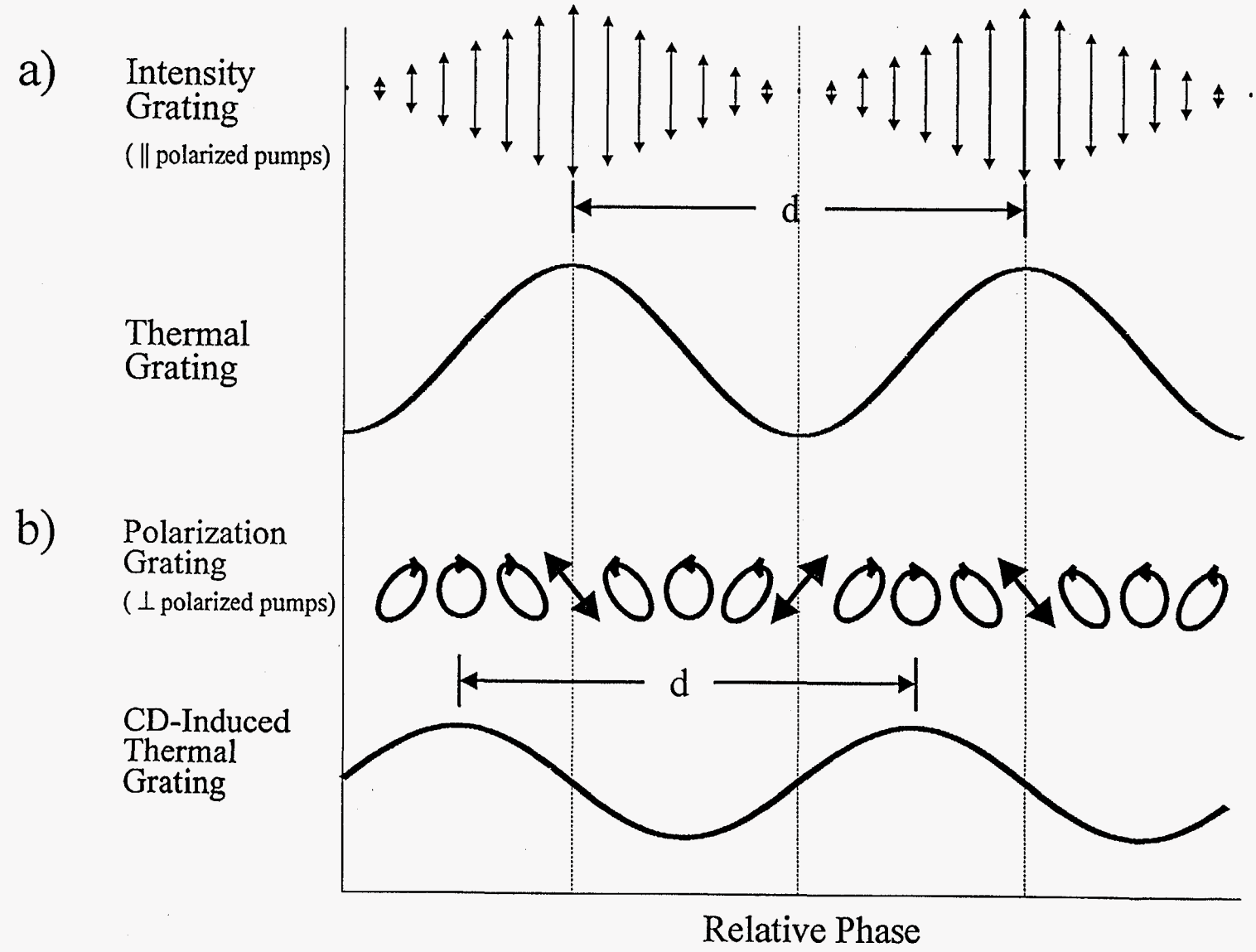
a)
Intensity Grating
(‖ polarized pumps)
d
Thermal Grating
b)
Polarization Grating
(⊥ polarized pumps)
d
CD-Induced Thermal Grating
Relative Phase

Figure 2

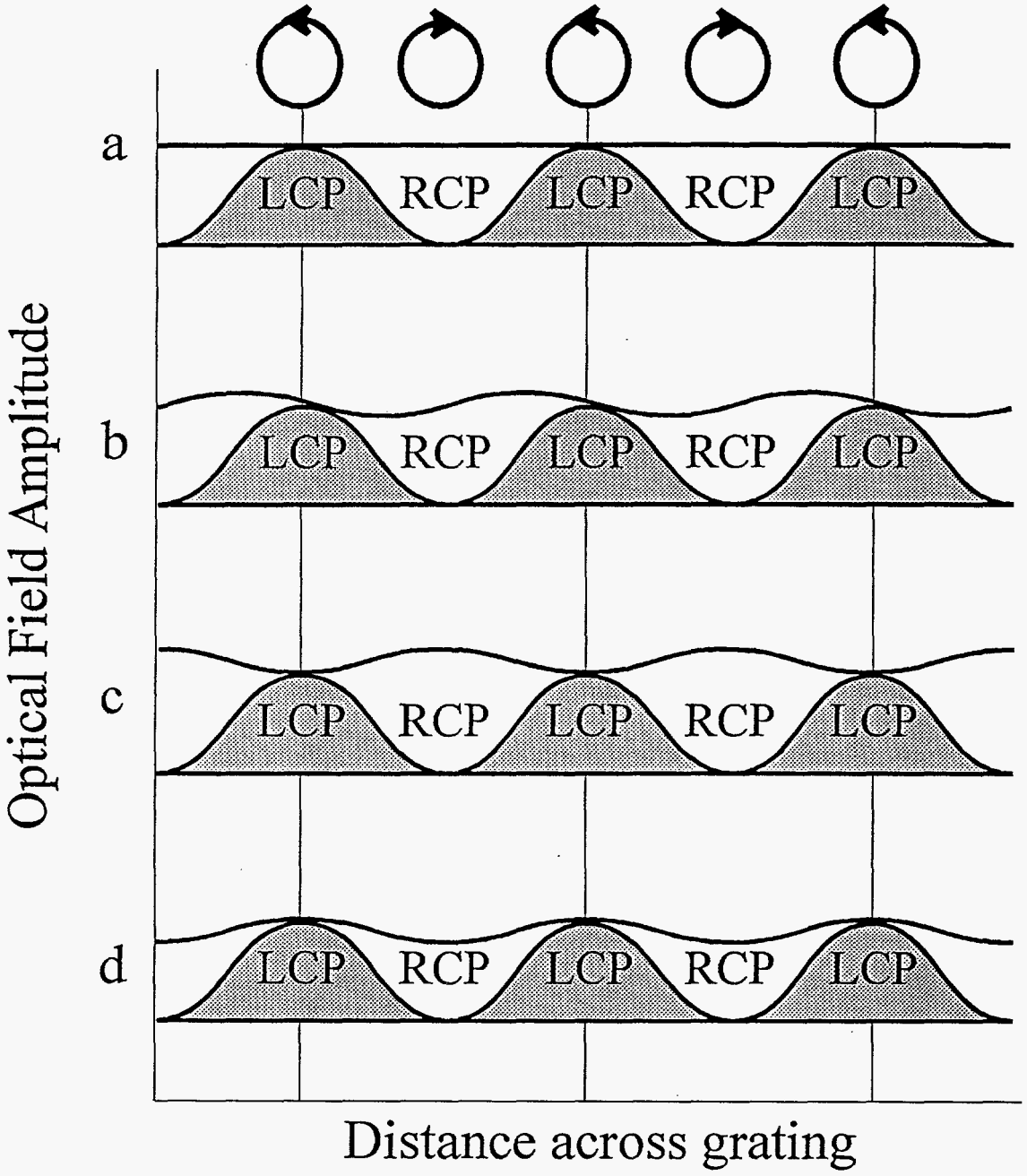
a
b
c
d
LCP
RCP
LCP
RCP
LCP
Optical Field Amplitude
Distance across grating

Figure 3

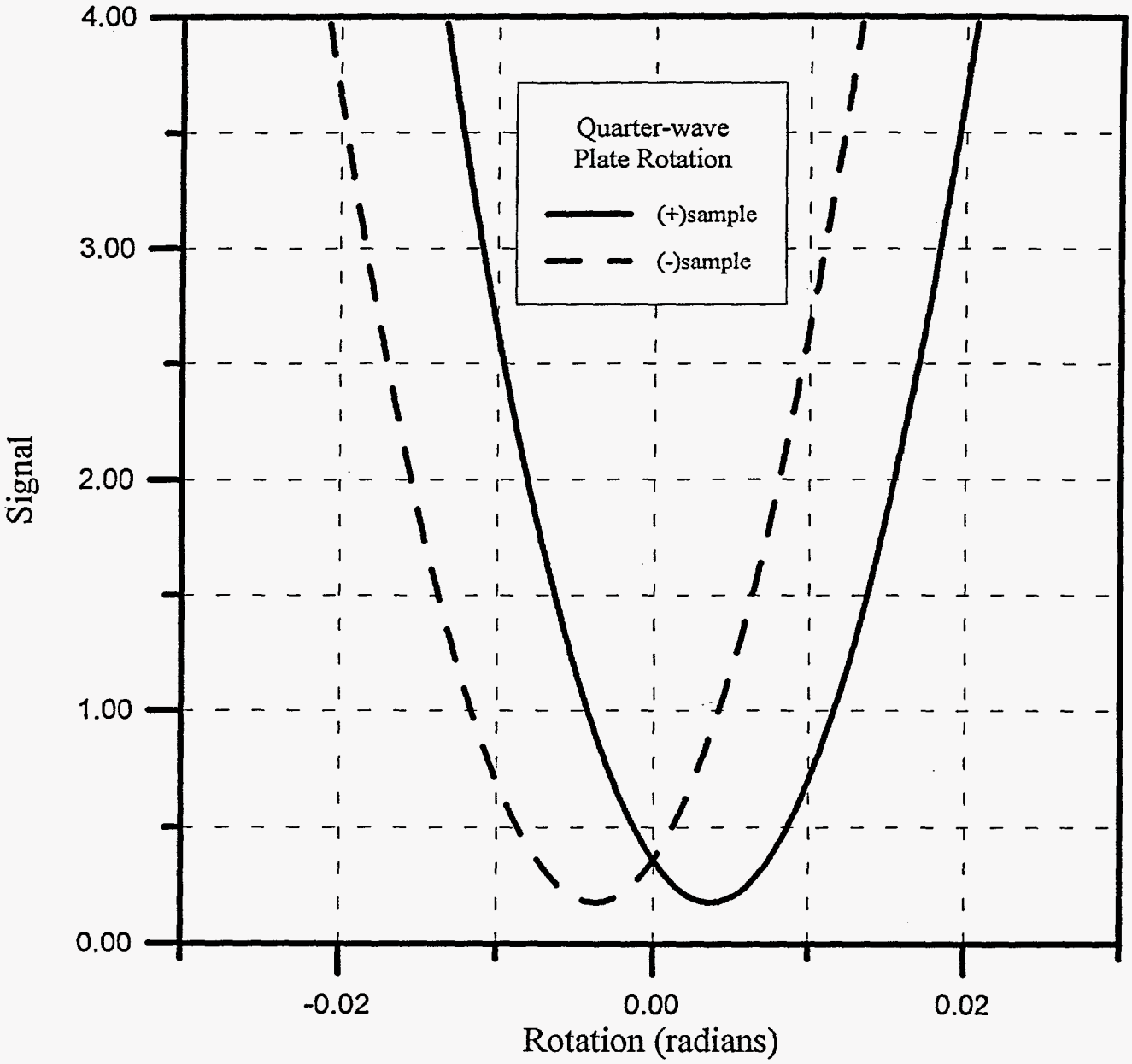
4.00
3.00
2.00
1.00
0.00
Signal
Quarter-wave
Plate Rotation
(+)sample
(-)sample
-0.02
0.00
0.02
Rotation (radians)

Figure 4

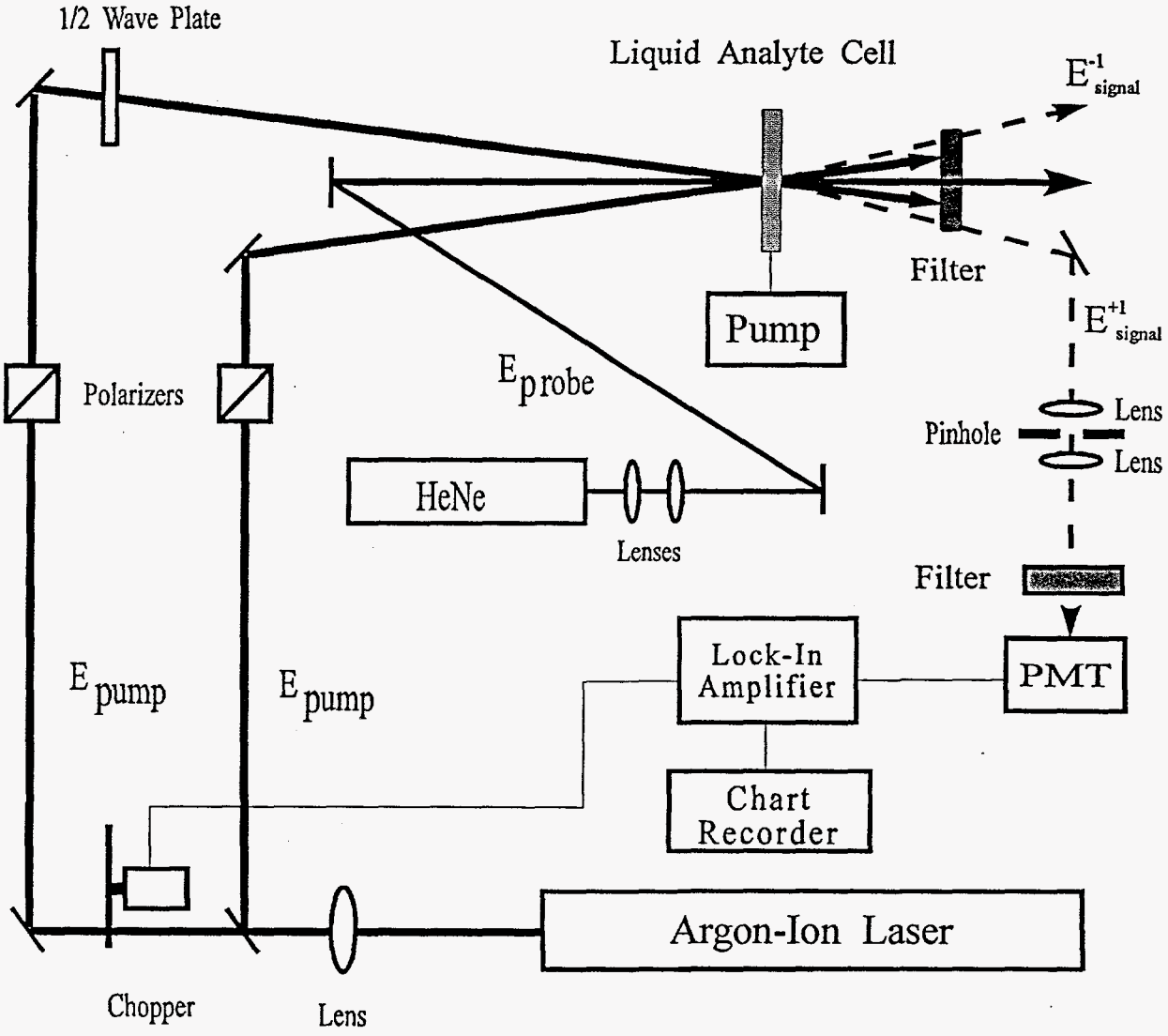
1/2 Wave Plate
Liquid Analyte Cell
E^{-1}_{signal}
Filter
Pump
E^{+1}_{signal}
Polarizers
E_{probe}
Pinhole
Lens
Lens
HeNe
Lenses
Filter
E_{pump}
E_{pump}
Lock-In Amplifier
PMT
Chart Recorder
Argon-Ion Laser
Chopper
Lens

Figure 5

UNLIMITED RELEASE

INITIAL DISTRIBUTION

San Diego State University
Department of Chemistry
ATTN: J. A. Nunes (10)
W. G. Tong (10)
San Diego, California 92182

D. W. Chandler, Sandia, 8353, MS 9055 (10)
L. A. Rahn, Sandia, 8351, MS 9057
F. P. Tully, Sandia, 8353 MS 9055
C. Meyers, 1011, MS 0320

MS 9001 J. C. Crawford, 8000
ATTN: E. E. Ives, 5200, MS 9006
J. B. Wright. 5300, MS 9005
M. E. John, 8100, MS 9004
R. L. Detry, 8200, MS 9037
L. A. Hiles, 8400, MS 9105
P. N. Smith, 8500, MS 9002
L. A. West, 8600, MS 9223
R. C. Wayne,8700, MS 9401
T. M. Dyer, 8800, MS 9141
D. L. Crawford, 8900, MS 9003

MS 9054 W. J. McLean, 8300
ATTN: W. G. Wolfer, 8341, MS 9161
R. H. Stulen, 8342, MS 9161
A. E. Pontau, 8347, MS 9162
G. A. Fisk, 8355, MS 9056
D. R. Hardesty, 8361, MS 9052
J. O. Keller, 8362, MS 9053
C. M. Hartwig, 8366, MS 9053

8535 Publications for OSTI (10)
8535 Publications/Technical Library Processes, 7141
7141 Technical Library Processes Department (3)
8523-2 Central Technical Files (3)